Sub Topic: Heterogeneous Combustion, Sprays & Droplets

9th U. S. National Combustion Meeting
Organized by the Central States Section of the Combustion Institute
May 17-20, 2015
Cincinnati, Ohio

Ultrafine Manganese Oxide Nanoparticles Synthesized by Flame Stabilized on a Rotating Surface

Joaquin Camacho, Changran Liu, Nicholas Montes, and Hai Wang*

High-Temperature Gas Dynamics Laboratory, Mechanical Engineering Department, Stanford University, Stanford, CA 94304
**Corresponding Author Email: jocamach@stanford.edu*

Abstract: The oxidation state and particle size are key properties that impact the electrochemical pseudocapacitance of manganese oxide nanoparticles. In this work, ultrafine manganese oxide nanoparticles were synthesized by the technique of flame stabilized on a rotating surface. Methylcyclopentadienyl manganese tricarbonyl (MMT) precursor was oxidized in a premixed fuel-lean flame (3.9% ethylene-29.5% oxygen-argon, equivalence ratio = 0.4). The particles are produced in the flame (T > 2000 K) and are transported largely by thermophoresis to the 400 K rotating substrate. The deposited samples were analyzed for their particle size distributions, crystal phase and oxidation state. Analysis by TEM shows that the particle size distributions have median diameter of 11 and 13 nm for 550 and 1150 ppm precursor concentrations, respectively. For these precursor loadings, the overall equivalence ratio of the unburned gas increases only slightly. The oxidation state of manganese in as-prepared manganese oxide particles was Mn(III) oxide at 550 ppm precursor concentration and a mixture of Mn(II) and Mn(III) at 1150 ppm, as indicated by X-ray diffraction. In contrast, the preferred oxidation state at the substrate temperature of 400 K is Mn(IV) from thermodynamic considerations, indicating that the oxidation state of the nanoparticles synthesized is controlled kinetically by the local flame condition as the particles are transported to the substrate. The as-synthesized nanoparticles were treated in air from 373 to 873 K from 3 hours to 3 months. The nanoparticle film did not oxidize from the Mn(III) oxidation state to Mn(IV) under all conditions, even though Mn(IV) is thermodynamically favored below 500K. The Mn(II) in nanoparticles comprised of a mixture Mn(II) and Mn(III) was however oxidized to Mn(III) at temperatures above 500K.

Keywords: Flame Synthesis, Nanoparticles, Metal Oxides

1. Introduction

Manganese oxide nanoparticles are useful in novel designs for devices such as batteries, solar cells, catalysts and biomedical probes. For example, ruthenium oxide nanopariticles are known to have the highest psuedocapacitance but manganese oxide is a more economical and ecological alternative for supercapacitor electrodes [1]. Many synthesis techniques have been employed to obtain manganese oxide nanoparticles with a range of particle sizes, morphology, crystal phase and oxidation state. In this work, the flame stabilized on a rotating surface (FSRS) technique, which was developed for efficient synthesis of TiO_2 nanoparticles [2-4] and TiO_2 mesoporous thin films [5-7], is utilized. It was demonstrated in previous studies that the FSRS technique carries several advantages in the fabrication of high-performance chemical sensors [7] and dye-sensitized solar cell anodes [8, 9]. Advantages of the FSRS techniques for manganese oxide nanoparticle synthesis will be demonstrated in this work.

The FSRS technique can potentially be used to control the particle size and crystal phase of manganese oxide nanoparticles. In the technique, a premixed laminar flame is stabilized by flow stretch close to the point of flow stagnation. A stable and uniform particle synthesis domain is confined within a narrow pseudo one-dimensional flow field between the flame and the stagnation/deposition surface [10]. The metal precursor in the form of a vaporized organometallic compound is carried by the unburned gas and precursor dissociation occurs in the preheat region of the flame. The metal vapor is oxidized in the flame followed by particle nucleation and mass/size growth by surface reaction and coagulation. Particle deposition onto the substrate is driven by the thermophoretic force resulting from the large temperature gradient (>3000 K/cm) between the flame and the stagnation/deposition surface. A controllable ultra-fine size with a narrow distribution is achieved due to the resulting thermophoretic velocity [11] which limits the growth to a few milliseconds [5]. In addition, the crystal phase of TiO_2 was controlled by the particle size and/or flame stoichiometry. In this work, we demonstrate that the FSRS technique is also suitable for manganese oxide nanoparticle synthesis with potential applications to electrochemical psuedocapacitors.

Manganese oxide nanoparticles synthesized by FSRS are studied here to determine the effect of precursor loading. Particle size, crystal phase, morphology and oxidation state are characterized as a function of precursor loading. Our primary objective is to assess the capability

of the FSRS method with respect to the range of particle properties the technique can access. The advantages to applying this method to the fabrication of manganese oxide based supercapacitor electrodes will also be discussed.

2. Experimental

The FSRS technique has been described in detail in previous studies [5-7]. To summarize, the burner is an aerodynamically shaped nozzle with a 1cm exit diameter which forms a laminar, premixed flat jet. The flow impinges on a stainless steel disc 30.4 cm in diameter which is mounted on a stepper motor 2.5 cm away from the burner nozzle. The disc rotates at 300 rpm which is above the threshold velocity for creating a boundary layer thickness smaller than the flame-to-surface distance and this eliminates flame perturbation [5]. At atmospheric pressure, a round flame about 2 cm in diameter is stabilized around 0.3 cm from the disc surface by flow stretch. The stagnation/deposition surface is 400K as measured by a type K thermocouple. A shroud of nitrogen gas flowing at 40 cm/s isolates the flame from the surrounding air.

The flame is 3.9% ethylene and 29.5% oxygen by volume with argon balance. The equivalence ratio is 0.4 before the precursor is added but it only changes slightly at the small precursor loading. The gas flow rates are metered individually by orifices operating above choked velocity conditions. The methylcyclopentadienyl manganese tricarbonyl (MMT) precursor (Sigma-Aldrich) was injected into the unburned mixture by syringe pump (Harvard PHD 2000 Infusion) and subsequently vaporized in the gas lines which were kept above 410K. The MMT precursor loadings used were 550 and 1150 ppm.

The synthesized manganese oxide nanoparticles were analyzed by X-ray diffraction (XRD) and transmission electron microscopy (TEM). XRD measurements were carried out on microscope slides upon which the film was directly deposited. A PANalytical X'pert Pro diffractometer was used with a Cu X-ray tube operating at 45 kV and 40 mA. The beam was conditioned by an X-ray mirror and a Ni beam attenuator. The diffracted beam is collected with a parallel plate collimator and a proportional photon detector. Diffraction patterns were obtained at 0.05 degrees per step and 1 second per step for films from both precursor loadings. For TEM analysis, the particles were collected by scraping the deposited film off the substrate and dispersing the particles by sonication in ethanol. The dispersed particle suspension was then deposited onto a copper-supported holey carbon TEM grid (Electron Microscopy Sciences

HC200-Cu) and dried. An FEI Tecnai G2 F20 X-Twin TEM with 200kV operating voltage is used to obtain medium resolution images and to observe crystal lattice spacing under high resolution.

3. Results and Discussion

Morphology and particle size of the as synthesized manganese oxide nanoparticles were characterized for two precursor loadings. The TEM images for nanoparticles synthesized at the 550 ppm precursor loading are shown in Fig. 1 at low and high resolution.

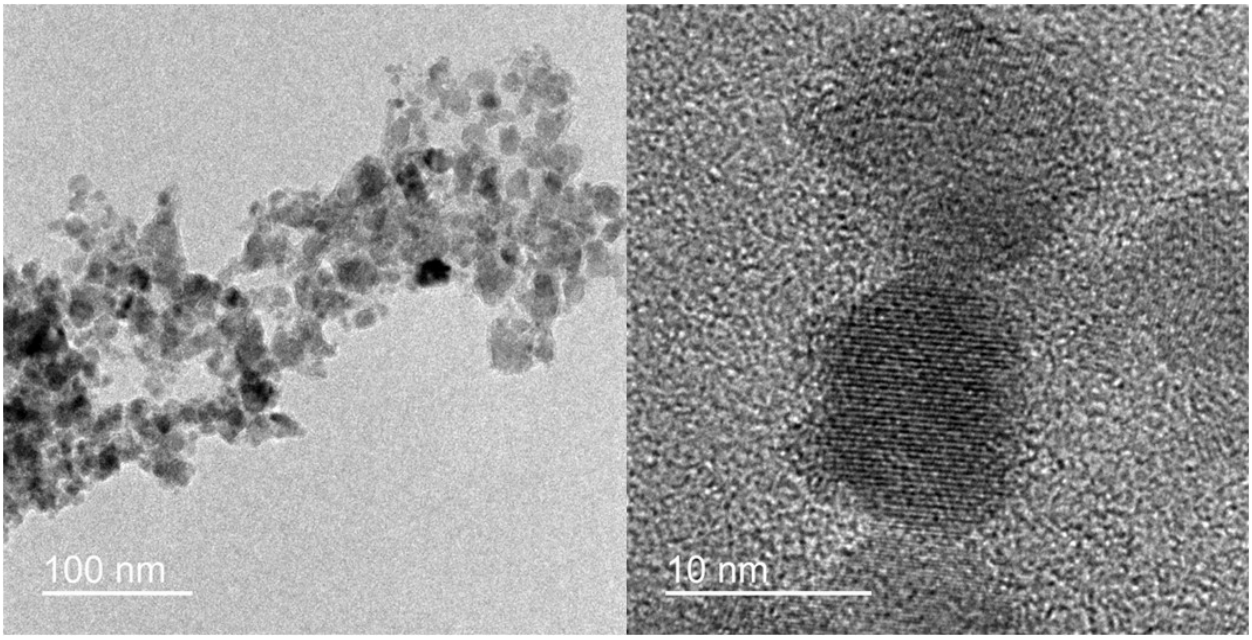

Figure 1: TEM images of nanoparticles synthesized at 550 ppm precursor loading at low (left plot) and high (right plot) resolution

As the figure shows, the particles are single crystals around 10 nm in size. The high resolution image in Fig. 1 shows that the particle has definitive lattice spacing. Images obtained by TEM for the nanoparticles formed at the 1150 ppm precursor concentration are shown in Fig. 2. The particle shape observed is less round compared to the lower precursor loading. At high resolution, regular lattice spacing is also observed but the polygonal shape is in stark contrast with the more round shape of the particles prepared at the lower precursor loading.

Particle size distributions were obtained from the TEM images. The non-spherical particle size was characterized from a 2-D circle that encircles the individual particle. The particle size distribution measured for both precursor loadings are shown in Fig. 3 for 200 particles sizes counted in each precursor loading. As expected, the particle size is smaller for the 550 ppm

precursor loading than the higher loading. The concentration is two time higher but the coagulation growth is expected to cause an increase of diameter by the cubic root of two.

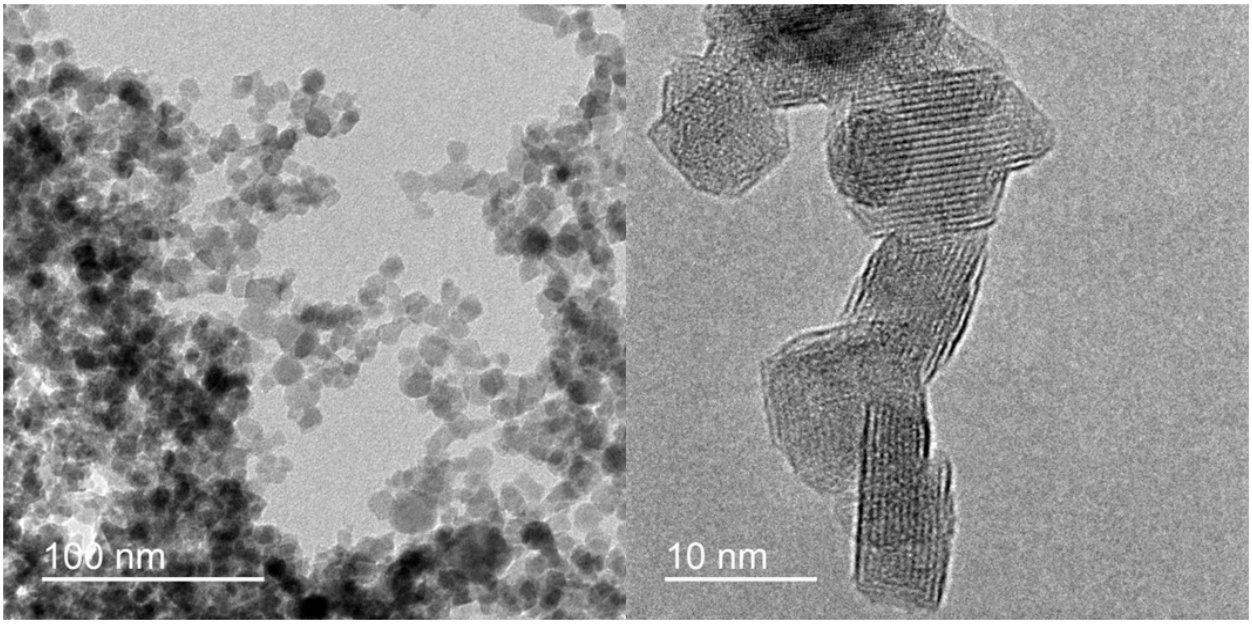

Figure 2: TEM images of nanoparticles synthesized at 1150 ppm precursor loading at low (left plot) and high (right plot) resolution

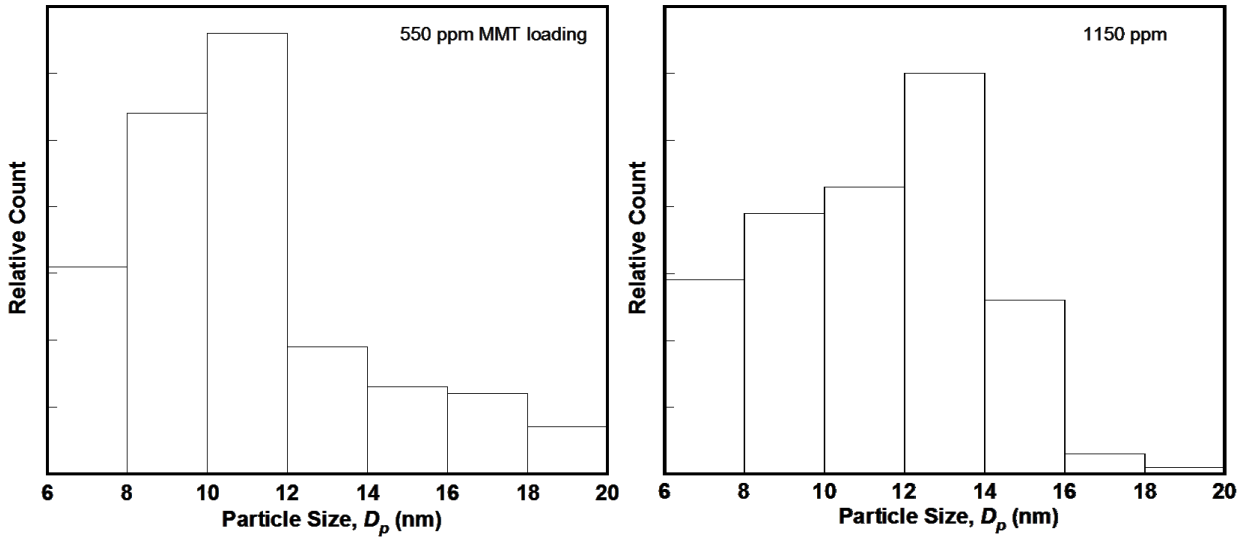

Figure 3: Particle size distributions measured for precursor loadings of 550 ppm (left plot) and 1150 ppm (right plot) for 200 particles each.

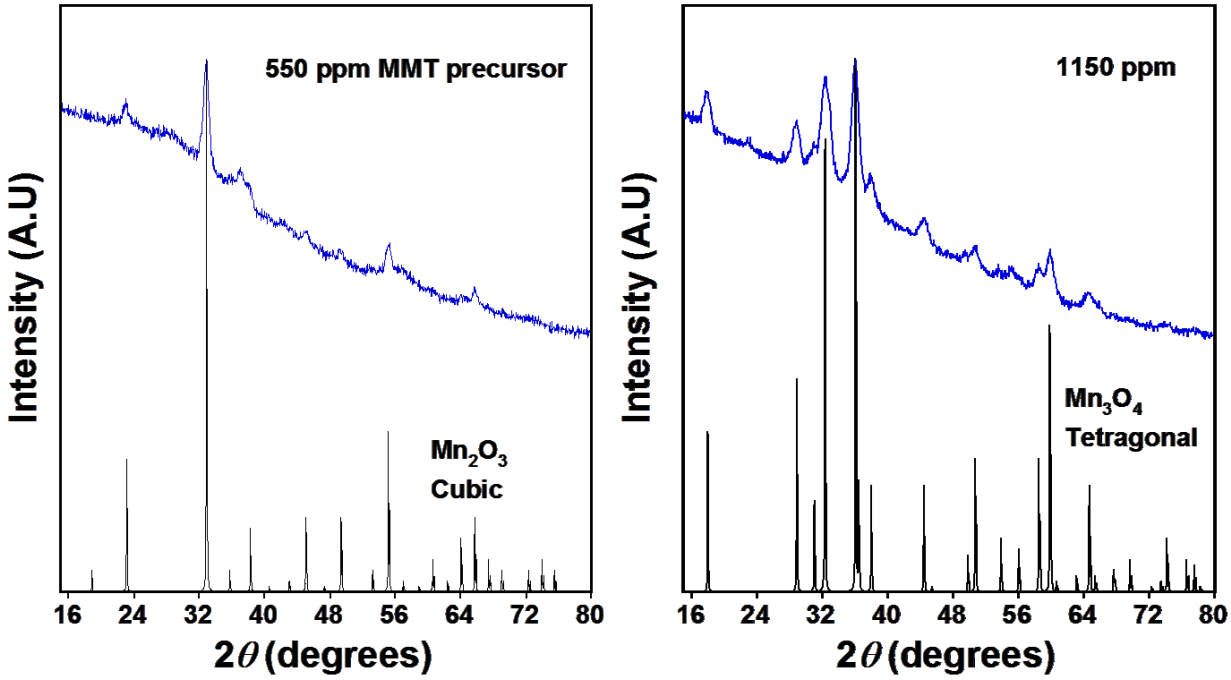

Figure 4:XRD patterns for as synthesized films of manganese oxides at 550 (left plot) and 1150 ppm (right plot) compared to standard PDFs of cubic Mn_2O_3 and tetragonal Mn_3O_4, respectively.

The crystal phase and oxidation state was examined by XRD to determine the effect of precursor loading on the synthesis products. The XRD patterns for the 550 and 1150 ppm MMT precursor loadings, shown in Fig. 4, are matched with standard Powder Diffraction Files (PDF). The crystal structures of the two samples differ: at the lower MMT loading the particles are cubic Mn_2O_3 (or Mn(III) oxide) while at the higher MMT loading, they are tetragonal Mn_3O_4 (or Mn(II,III) oxide). It is important to note that all synthesis conditions are the same except for the precursor loading, which is small and does not perturb the equivalence ratio of the flame to a significant extent. Furthermore, the oxygen concentration is always in excess.

The observations made above cannot be explained solely by thermodynamic arguments. The phase equilibria between the oxides of manganese nanoparticles are known. In fact, the Mn(IV) oxide product is favored below 500 K in an oxidizing environment [12], and this is the condition close to the stagnation surface. In contrast, the Mn(II) and Mn(III) oxidation states are favored at higher temperatures. The fact that the as-synthesized particles are in the more reduced oxidation states indicates that the solidification process at a temperature higher than 500 K dictates the particle oxidation state. That is, as the particles are transported from the high temperature flame region (> 2000 K) towards the cold stagnation surface, they solidify, and the

oxidation of Mn(II) and MN(III) below 500 K must be too slow to convert the particles to the Mn(IV) oxidation state.

To support the above argument, the synthesized films were further treated to determine whether the as-prepared films can be oxidized further. The films were heated at temperatures ranging from 373 to 837K in an ambient pressure air environment. The films were then examined by XRD to determine any change in their crystal phase and oxidation state. The XRD patterns for Mn_2O_3 films (550 ppm loading) are shown in Fig. 5. According to the observed diffraction patterns, no oxidation or change in crystal structure occurred over the entire range of temperatures. Annealing and grain growth were the only changes observed at higher temperatures, as evidenced by the narrowed XRD peaks. In addition, the thermodynamically predicted oxidation from Mn(III) oxide to Mn(IV) oxide in air at 473K [12] was not observed even after 3 months of heating, indicating that it is nearly impossible to convert the flame-synthesized nanoparticles of Mn(III) from its meta-stable thermodynamic state to the Mn(IV) state.

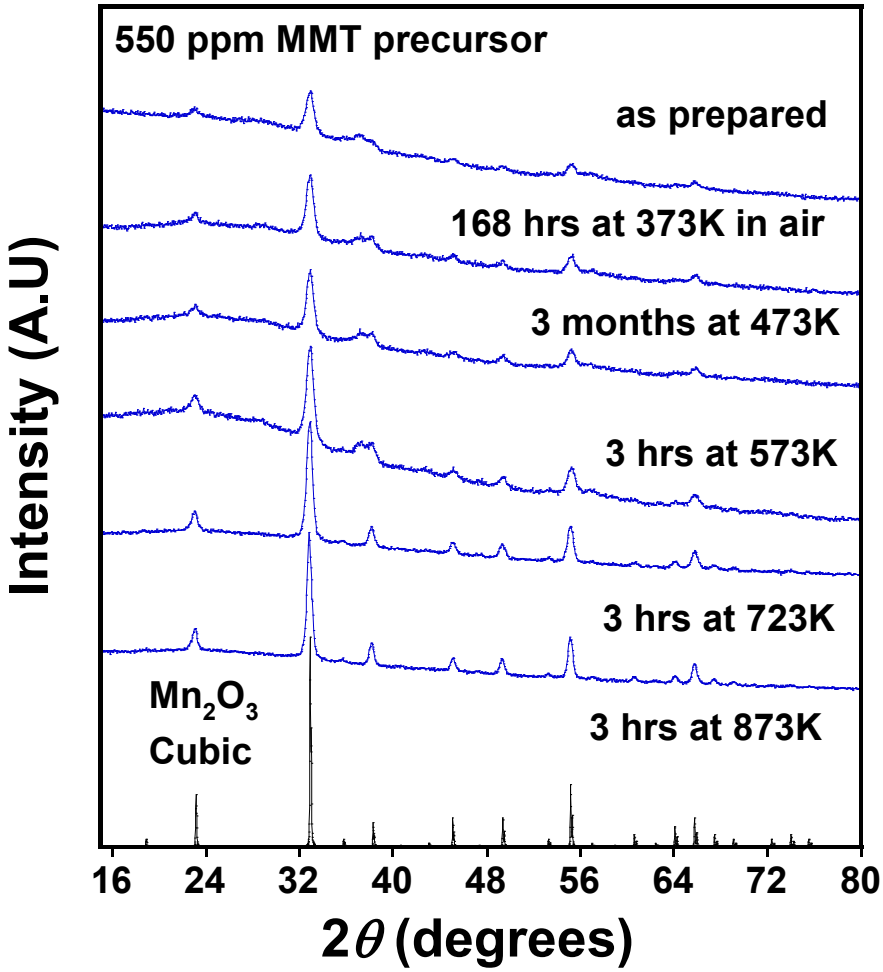

Figure 5. XRD patterns of the Mn(III) oxide after heat treatment in air.

Heat treatment of the Mn(II,III) oxide nanoparticle film was also carried out for the same conditions. The observed diffraction patterns are shown in Fig. 6. Unlike the Mn(III) oxide film shown above, the Mn(II,III) oxide is oxidized to Mn(III) oxide after heating in air at temperatures equal to or higher than 773 K. Above 373K, there is a visible change in the crystal structure which corresponds to a mixture of the two crystal phases. At 573K, it only takes 3 hours for the XRD pattern to resemble Mn(III) oxide. At 723 K and above, oxidation to Mn(III) oxide readily occurs along with crystal grain growth.

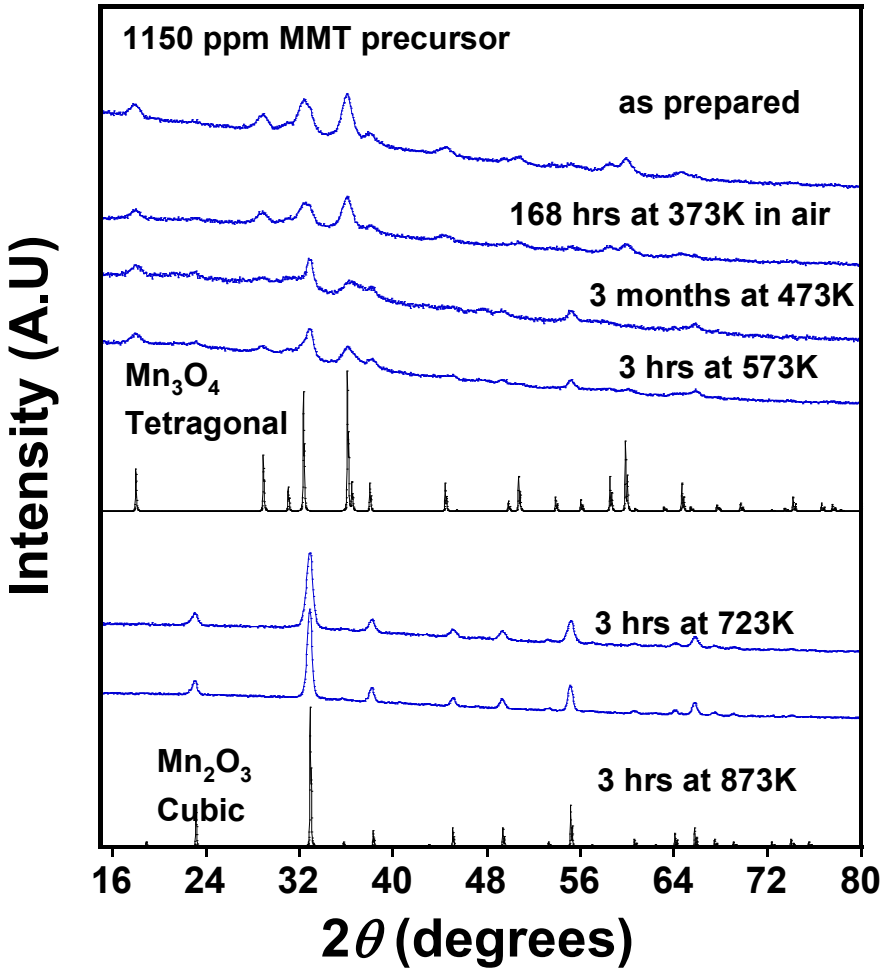

Figure 6. XRD patterns of Mn(II,III) oxide after heat treatment in air.

Clearly, the advantages of the FSRS synthesis method reported previously also carry over to the synthesis of manganese oxides. The control of particle size and oxidation state reported here may be useful in the optimization of supercapacitor electrode designs. The sensitivity of supercapacitor performance to the oxidation state of manganese will be explored in future works. In addition, the particle size and morphology are design parameters that must be controlled and applied to improve the performance of the supercapacitor electrodes.

4. Conclusions

Ultrafine manganese oxide nanoparticles were synthesized by the technique of flame stabilized on a rotating surface. MMT precursor was oxidized in a premixed fuel-lean ethylene flame and the particle products were deposited as nanoparticle films. Analysis by TEM shows that the particle size distributions have median diameter of 11 and 13 nm for 550 and 1150 ppm

precursor concentrations, respectively. The oxidation states of manganese in as-prepared manganese oxide particles are Mn(III) oxide at 550 ppm precursor concentration and a mixture of Mn(II) and Mn(III) at 1150 ppm, as indicated by XRD. In contrast, the thermodynamically preferred oxidation state is Mn(IV) at the substrate temperature of 400 K, indicating that the oxidation state of the nanoparticles synthesized is controlled kinetically by the local flame condition as the particles are transported to the substrate. The as-synthesized nanoparticles were treated in air from 373 to 873 K from 3 hours to 3 months. The nanoparticle film did not oxidize from the Mn(III) oxidation state to Mn(IV) under all conditions, even though Mn(IV) is thermodynamically favored below 500K. The Mn(II) nanoparticles comprised of a mixture Mn(II) and Mn(III) was however oxidized to Mn(III) at temperatures above 500K.

6. References

[1] W. Wei, X. Cui, W. Chen, D. G. Ivey, Chem. Soc. Rev. 40 (2011) 1697-1721.

[2] J. R. McCormick, B. Zhao, S. A. Rykov, H. Wang, J. G. Chen, J. Phys. Chem. B 108 (2004) 17398-17402.

[3] B. Zhao, K. Uchikawa, J. R. McCormick, C. Y. Ni, J. G. Chen, H. Wang, Proc. Combust. Inst. 30 (2005) 2569-2576.

[4] B. Zhao, K. Uchikawa, H. Wang, Proc. Combust. Inst. 31 (2007) 851-860.

[5] E. D. Tolmachoff, A. D. Abid, D. J. Phares, C. S. Campbell, H. Wang, Proc. Combust. Inst. 32 (2009) 1839-1845.

[6] S. Memarzadeh, E. D. Tolmachoff, D. J. Phares, H. Wang, Proc. Combust. Inst. 33 (2011) 1917-1924.

[7] E. Tolmachoff, S. Memarzadeh, H. Wang, J. Phys. Chem. C 115 (2011) 21620-21628.

[8] S. Nikraz, D. J. Phares, H. Wang, J. Phys. Chem. C 116 (2012) 5342-5351.

[9] S. Nikraz, H. Wang, Proc. Combust. Inst. 34 (2013) 2171-2178.

[10] M. D. Smooke, I. K. Puri, K. Seshadri, Symp. (Int.) Combust. 21 (1986) 1783-1792.

[11] Z. G. Li, H. Wang, Phys. Rev. E 70 (2004) 021205.

[12] N. Birkner, A. Navrotsky, Am. Mineral. 97 (2012) 1291-1298.